

# Ti-Ni Shape Memory Alloys

T.W. Duerig and A.R. Pelton, Nitinol Development Corporation

This datasheet describes some of the key properties of equiatomic and near-equiatomic titanium-nickel alloys with compositions yielding shape memory and superelastic properties. Shape memory and superelasticity *per se* will not be reviewed; readers are referred to Ref 1 to 3 for basic information on these subjects. These alloys are commonly referred to as nickel-titanium, titanium-nickel, Tee-nee, Memorite™, Nitinol, Tinel™, and Flexon™. These terms do not refer to single alloys or alloy compositions, but to a family of alloys with properties that greatly depend on exact compositional make-up, processing history, and small ternary additions. Each manufacturer has its own series of alloy designations and specifications within the “Ti-Ni” range.

A second complication that readers must acknowledge is that all properties change significantly at the transformation temperatures  $M_s$ ,  $M_f$ ,  $A_s$ , and  $A_f$  (see figure on the right and the section “Tensile Properties”). Moreover, these temperatures depend on applied stress. Thus, any given property depends on temperature, stress, and history.

## Product Forms and Applications

Titanium-nickel is most commonly used in the form of cold drawn wire (down to 0.02 mm) or as barstock. Other commercially available forms not yet sold as standard product would include tubing (down to 0.3 mm OD), strip (down to 0.04 mm in thickness), and sheet (widths to 500 mm and thicknesses down to 0.5 mm). Castings (Ref 4), forgings and powder metallurgy (Ref 5) products have not yet been brought from the research laboratory.

**Typical Conditions.** Titanium-nickel is most commonly used in a cold worked and partially annealed condition. This partial anneal does not recrystallize the material, but does bring about the onset of recovery processes. The extent of the post-cold worked recovery depends on many aspects of the application, such as the desired stiffness, fatigue life, ductility, recovery stress, etc. Fully annealed conditions are used almost exclusively when a maximum  $M_s$  is needed. Although the cold worked condition does not transform and does not exhibit shape memory, it is highly elastic and has been considered for many applications (Ref 6).

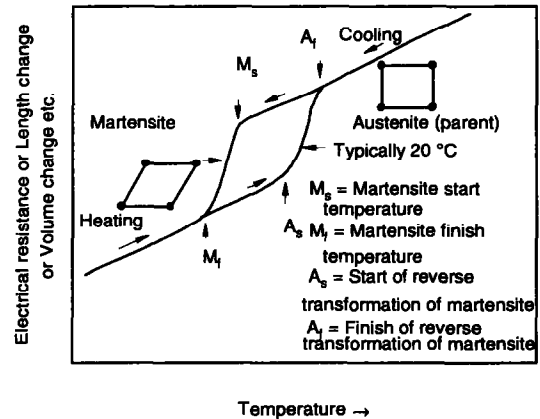
**Response to Heat Treatment.** Recovery processes begin at temperatures as low as 275 °C (525 °F). Recrystallization begins between 500 and 800 °C (930 and 1470 °F), depending on alloy composition and the degree of cold work.

Aging of unstable (nickel-rich) compositions begins at 250 °C (525 °F), causing the precipitation of a complex sequence of nickel-rich precipitates (Ref 7), as these products leach nickel from the matrix, their general effect is to increase the  $M_s$  temperature. The solvus temperature is about 550 °C

## Special Properties

Many shape memory-related properties are discussed in subsequent sections (transformation

## Effect of phase transformation



Schematic illustration of the effects on a phase transformation on the physical properties of Ti-Ni. All physical properties exhibit a discontinuity, characterized by the transformation temperatures shown.

Source: C.M. Wayman and T.W. Duerig, *Engineering Aspects of Shape Memory Alloys*, T.W. Duerig, et al., Ed., Butterworth-Heinemann, 1990, p 10

(1020 °F).

**Applications** for titanium-nickel alloys can be conveniently divided into four categories (Ref 8):

- **Free recovery (motion)** applications are those in which a shape memory component is allowed to freely recover its original shape during heating, thus generating a recovery strain (Ref 9).
- **Constrained recovery (force)** applications are those in which the recovery is prevented, constraining the material in its martensitic, or cold, form while recovering (Ref 9). Although no strain is recovered, large recovery stresses are developed. These applications include fasteners and pipe couplings and are the oldest and most widespread type of practical use.
- **Actuators (work)** applications are those in which there is both a recovered strain and stress during heating, such as in the case of a titanium-nickel spring being warmed to lift a ball (Ref 10). In these cases, work is being done. Such applications are often further categorized according to their actuation mode, e.g., electrical or thermal.
- **Superelasticity (energy storage)** refers to the highly exaggerated elasticity, or springback, observed in many Ti-Ni alloys deformed above  $A_s$  and below  $M_d$  (Ref 11). The function of the material in such cases is to store mechanical energy. Although limited to a rather small temperature range, these alloys can deliver over 15 times the elastic motion of a spring steel.

temperatures, superelasticity, etc.). Some properties, however, are strictly peculiar to shape mem-

1036 / Advanced Materials

ory alloys and cannot be conveniently categorized in standard outline forms. The more important of these properties are discussed below.

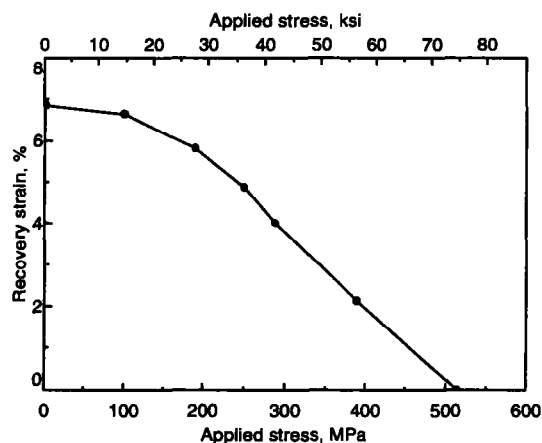
**Free-recoverable strain** in polycrystalline titanium-nickel can reach 8%, but is limited to a maximum of 6% if complete recovery is expected.

**Applied stresses** opposing recovery reduce recoverable strain. Clearly, stronger alloys will be affected less by opposing stresses. Work output is maximized at intermediate stresses and strains.

**Recoverable stresses** generally reach 80 to 90% of yield stress. In fact, alloy behavior depends on numerous factors, including the compliance of the resisting force and the constraining strain (Ref 9 and 12). Typical values are as follows:

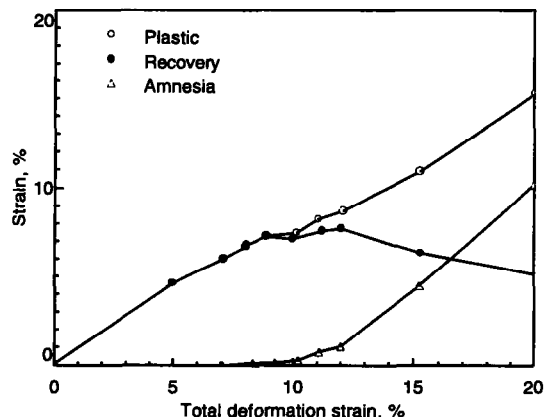
Condition	Recovery stress, MPa
Annealed barstock	400
Cold worked barstock annealed at 500 °C (930 °F)	700
Cold worked wire annealed at 400 °C (750 °F)	1000

Effects of opposing stresses on recovery strain



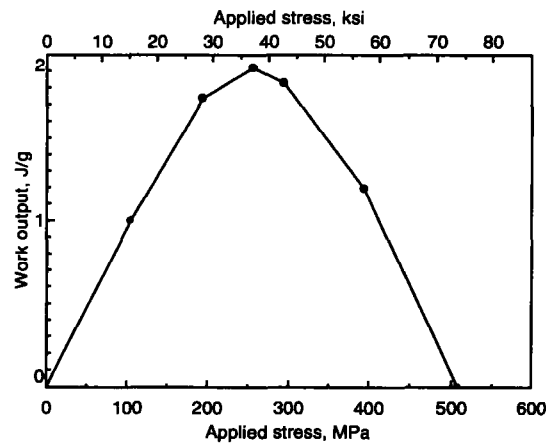
Ti-Ni-Fe barstock with 50 at.% Ni and 3% Fe fully annealed, tested in uniaxial tension. Source: J.L. Proft and T.W. Duerig, *Engineering Aspects of Shape Memory Alloys*, T.W. Duerig et al., Ed., Butterworth-Heinemann, London, 1990, p 115

Free recovery behavior



Ti-Ni-Fe barstock with 50 at.% Ni and 3% Fe fully annealed, tested in uniaxial tension. After deforming Ti-Ni to various total strains (x-axis), the material springs back to the plastic strain levels shown by the open circles. After heating above  $A_1$ , most of the strain is recovered, but some amnesia persists. The difference between the plastic strain and the amnesia is the recoverable strain (closed circles). Source: J.L. Proft and T.W. Duerig, *Engineering Aspects of Shape Memory Alloys*, T.W. Duerig et al., Ed., Butterworth-Heinemann, London, 1990, p 115

Work output of a Ti-Ni alloy



Ti-Ni-Fe barstock with 50 at.% Ni and 3% Fe in a work-hardened condition, tested in uniaxial tension. Source: J.L. Proft and T.W. Duerig, *Engineering Aspects of Shape Memory Alloys*, T.W. Duerig et al., Ed., Butterworth-Heinemann, London, 1990, p 115

Chemistry and Density

Density, 6.45 to 6.5 g/cm<sup>3</sup>

Titanium-nickel is extremely sensitive to the precise titanium/nickel ratio (see figure below). Generally, alloys with 49.0 to 50.7 at.% titanium are commercially common, with superelastic alloys in the range of 49.0 to 49.4 at.% and shape

memory alloys in the range of 49.7 to 50.7 at.%. Binary alloys with less than 49.4 at.% titanium are generally unstable. Ductility drops rapidly as nickel is increased.

Binary alloys are commonly available with  $M_s$

temperatures between  $-50^{\circ}$  and  $+100^{\circ}\text{C}$  ( $-58$  to  $212^{\circ}\text{F}$ ). Commercially available ternary alloys are available with  $M_s$  temperatures down to  $-200^{\circ}\text{C}$  ( $-330^{\circ}\text{F}$ ). Titanium-nickel is also quite sensitive to alloying additions.

**Oxygen** forms a  $\text{Ti}_4\text{Ni}_2\text{O}_x$  inclusion (Ref 13), tending to deplete the matrix in titanium, lower  $M_s$ , retard grain growth, and increase strength. Levels usually are controlled to  $<500$  ppm. Nitrogen forms the same compound and has an additive effect to oxygen.

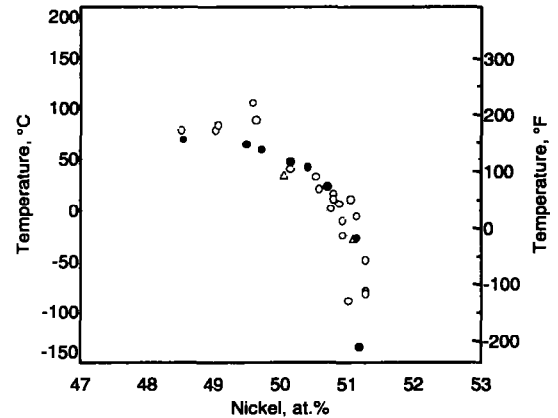
**Fe, Al, Cr, Co, and V** tend to substitute for nickel, but sharply depress  $M_s$  (Ref 14 to 16), with V and Co being the weakest suppressants and Cr the strongest. These elements are added to suppress  $M_s$  while maintaining stability and ductility. Their practical effect is to stiffen a superelastic alloy, to create a cryogenic shape memory alloy, or to increase the separation of the R-phase from martensite.

**Pt and Pd** tend to decrease  $M_s$  in small quantities ( $\sim 5$  to  $10\%$ ), then tend to increase  $M_s$ , eventually achieving temperatures as high as  $350^{\circ}\text{C}$  ( $660^{\circ}\text{F}$ ) (Ref 17).

**Zr and Hf** occasionally have been reported to increase  $M_s$ , but are generally neutral when substituted for titanium on an atomic basis.

**Nb and Cu** are used to control hysteresis and

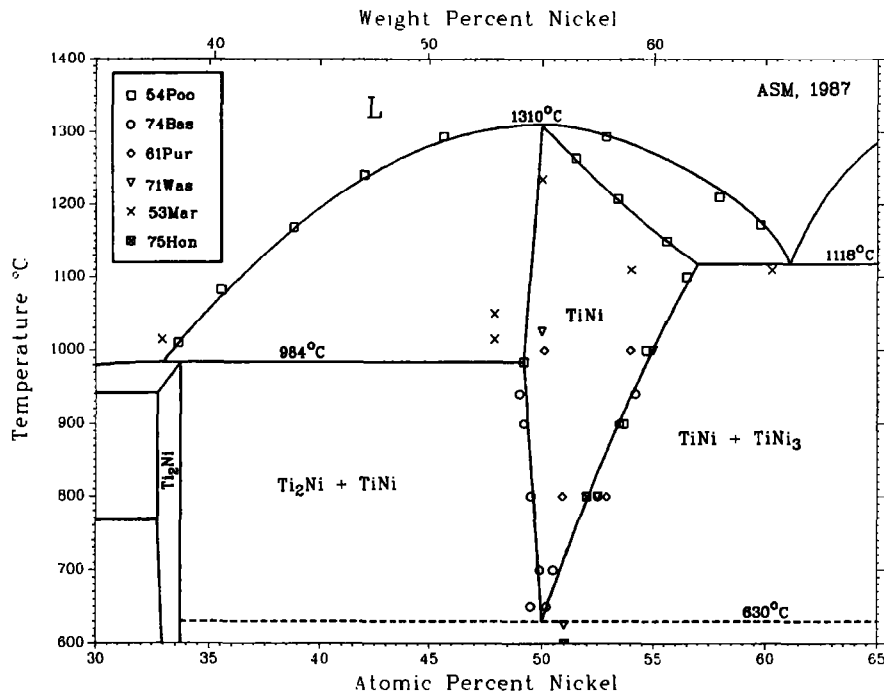
Effect of composition on  $M_s$



$M_s$  temperatures in nickel-titanium alloys are extremely sensitive to compositional variation, particularly at higher nickel contents. Source: K.N. Melton, *Engineering Aspects of Shape Memory Alloys*, T.W. Duerig et al., Ed., Butterworth-Heinemann, 1990, p 10

martensitic strength. Nb is added to increase hysteresis (desirable for coupling and fastener applications), and copper (Ref 19) is added to reduce hysteresis (for actuator applications).

Central Portion of Ti-Ni Phase Diagram



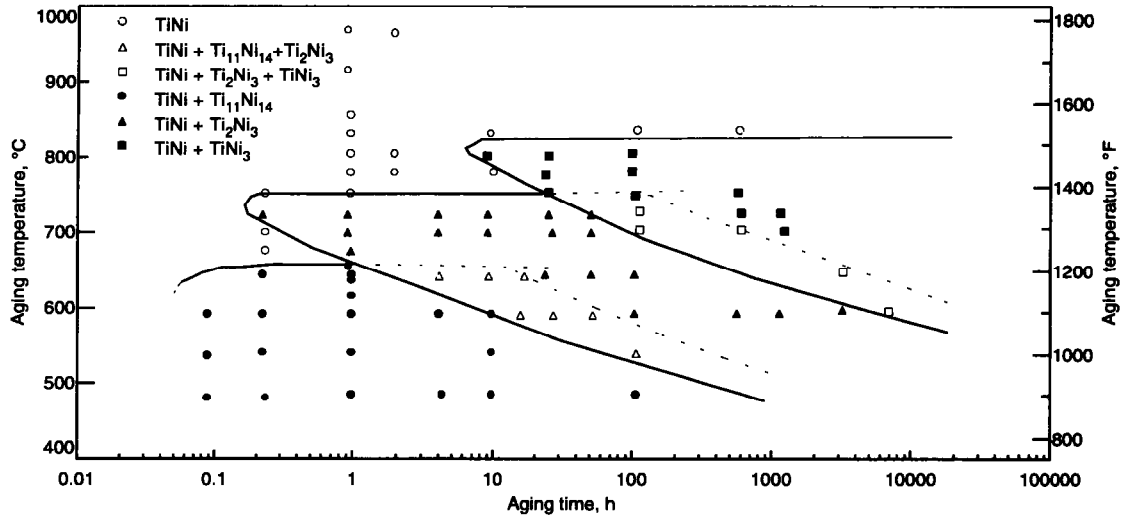
Phases and Structures

Crystal Structure

The high-temperature austenitic phase ( $\beta$ ) has a  $B_2$ , or  $\text{CsCl}$  ordered structure with  $a_0 = 3.015 \text{ \AA}$ . The most common martensitic structure ( $B19'$ ) has a complex monoclinic structure with  $a = 2.889 \text{ \AA}$ ,  $b = 4.120 \text{ \AA}$ ,  $c = 4.622 \text{ \AA}$ , and  $\beta = 96.8^{\circ}$  (Ref 20). The  $M_s$  can range from  $<-200$  to  $+100^{\circ}\text{C}$  ( $-328$  to  $212^{\circ}\text{F}$ ). It

is worth noting that there is also a "transition" structure that preceded the martensite, called the R-phase with a rhombohedral structure (Ref 21). Although this R phase exhibits a number of interesting properties, it will not be reviewed extensively here.

Time-temperature-transformation curve



Time-temperature-transformation curve for Ti-51Ni, which shows precipitation reactions as a function of temperature and time. Source: M. Nishida, C.M. Wayman, and T. Honma, *Metall. Trans. A*, Vol 17, 1986, p 1505

**Transformation Products**

The T-T-T diagram shows the aging reactions in unstable (>50.6% Ni) titanium-nickel alloys (Ref 7). In general,  $TiNi \rightarrow Ti_{11}Ni_{14} \rightarrow Ti_2Ni_3 \rightarrow TiNi_3$  as the aging temperature increases or as

time increases at a constant temperature. These precipitation reactions can be readily monitored via transformation temperature or mechanical-property measurements.

**Physical Properties**

**Damping Characteristics**

Internal friction and damping of titanium-nickel alloys are dramatically affected by temperature changes (see figure on left). Cooling (or heating) produces peaks, which correspond to the transformation temperatures. At higher temperatures, a very sharp increase is observed during

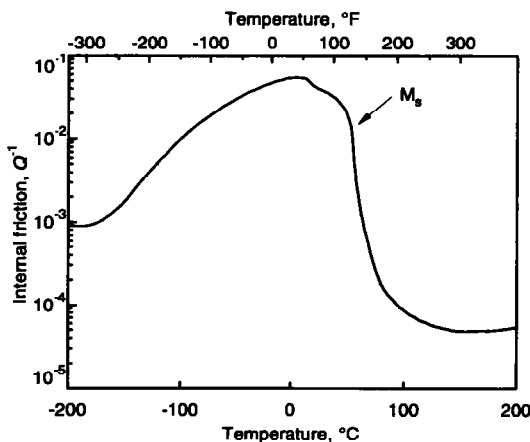
cooling through the  $M_s$ . These usually high damping characteristics (Ref 22) have been studied for some time, but have not been used on a commercial basis due to their limited temperature range and rapid fatigue degradation.

**Elastic Constants**

Dynamically measured moduli (Ref 23 and 24) change markedly with the martensitic transformation and premartensitic effects (see figure on

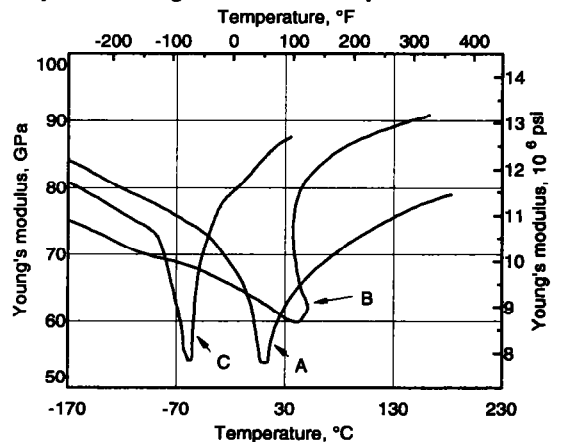
right). Typical values of elastic moduli are 40 GPa ( $5.8 \times 10^6$  psi) for martensite and 75 GPa ( $10.8 \times 10^6$  psi) for austenite. From a practical point of

Ti-Ni-Cu alloy damping characteristics



Internal friction of 44.7Ti-29.3Ni-26 Cu (wt%) during cooling with measurement frequency of -1 Hz. Source: O. Mercier and E. Török, *J. Phys.*, Vol C-4 (No. 43), 1982, p C-4270

Dynamic Young's modulus vs temperature



A: Ti-55Ni (wt%). B: 44.7Ti-29.3Ni-26Cu (wt%). C: 44.9Ti-51.7Ni-3.4Fe (wt%). Source: O. Mercier, K.N. Melton, R. Gotthardt, and A. Kulik, *Proc. Int. Conf. Solid-Solid Phase Transformations*, H.I. Aaronson, D.E. Laughlin, R.F. Sekerka, and C.M. Wayman, Ed., AIME, 1982, p 1259

view, however, modulus is of little value; apparent elasticity is more controlled by the transformation and by mechanical twinning. Poisson's ratio,  $\mu$ , is 0.33 (Ref 25).

### Electrical Resistivity

General values for electrical resistivity of the two primary phases are as follows (Ref 26):

$$\rho \text{ (martensite)} = 76 \times 10^{-6} \Omega \cdot \text{cm}$$

$$\rho \text{ (austenite)} = 82 \times 10^{-6} \Omega \cdot \text{cm}$$

Variations in resistivity with temperature are complex functions of composition and thermomechanical processing (see figure). Note also the pronounced effect of the R-phase on resistivity.

### Magnetic Characteristics

Magnetic susceptibility also undergoes a discontinuity during phase transition (Ref 26). Typical values are:

$$\chi \text{ (martensite)} = 2.4 \times 10^{-6} \text{ emu/g}$$

$$\chi \text{ (austenite)} = 3.7 \times 10^{-6} \text{ emu/g}$$

## Corrosion

Titanium-nickel generally forms a passive  $\text{TiO}_2$  (rutile) surface layer (Ref 27). Like titanium alloys, there is a transition temperature of about 500 °C (930 °F), above which the oxide layer will be dissolved and absorbed into the material. Unlike titanium alloys, however, no  $\alpha$  case is formed. Titanium-nickel will also react with nitrogen during heat treatments, forming a TiN layer.

### General Corrosion

The rest potential of titanium-nickel in a dilute sodium chloride solution is around 0.23 V (SCE), which compares with 0.38 V for type 304 stainless steel. This puts titanium-nickel on the noble or protected side of stainless steel in the galvanic series. A passive oxide/nitride surface film is the basis of the corrosion resistance of titanium-nickel alloys, similar to stainless steels. Specific environments can cause the passive film to break down, thus subjecting the base material to attack. A summary of titanium-nickel reactions in various environments follows (Ref 28).

**Seawater.** Titanium-nickel is not affected when immersed in flowing seawater; however, in stagnant seawater, such as found in crevices, the protective film can break down, which results in pitting corrosion.

**Acetic acid** ( $\text{CH}_3\text{COOH}$ ) attacks titanium-nickel at a modest rate of  $2.5 \times 10^{-2}$  to  $7.6 \times 10^{-2}$  mm/year (mpy) over the temperature range 30 °C (86 °F) to the boiling point and over the concentration range 50 to 99.5%.

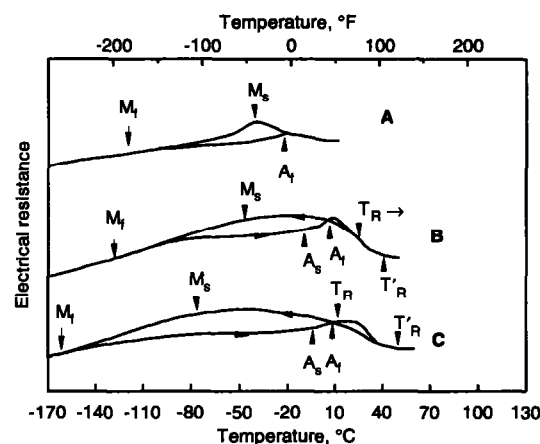
**Methanol** ( $\text{CH}_3\text{OH}$ ) appears to attack titanium nickel only when diluted with low concentrations of water and halides. This impure methanol solution leads to pitting and tunneling corrosion similar to that found in titanium alloys.

**Cupric chloride** ( $\text{CuCl}_2$ ) at 70 °C (160 °F) at-

### Hydrogen Damage

The interaction between hydrogen and titanium-nickel is sensitive to both concentration and temperature (Ref 31). In general, hydrogen levels

### Electrical resistance vs temperature



Electrical resistance vs temperature curves for a Ti-50.6Ni (at.%) alloy that was thermomechanically treated as indicated. A: Quenched from 1000 °C (1830 °F). B: Quenched from 1000 °C (1830 °F), aged at 400 °C (750 °F). C: Directly aged at 400 °C (750 °F).  $T_R$  is the transition temperature from austenite to the rhombohedral R phase.  $T'_R$  is the shifted transition temperature from processing effects. Arbitrary units for electrical resistance.

Source: S. Miyazaki and K. Otsuka, *Metall. Trans. A*, Vol 17, 1986, p 53

tacks titanium-nickel at 5.5 mpy.

**Ferric chloride** ( $\text{FeCl}_3$ ) at 70 °C (160 °F) and 8% concentration attacks titanium-nickel at 8.9 mpy. Titanium-nickel is attacked at a rate of 2.8 mpy in a solution of 1.5%  $\text{FeCl}_3$  with 2.5% HCl.

**Hydrochloric acid** (HCl) has a variety of effects on the corrosion of titanium-nickel alloys depending on temperature, acid concentration, and specific alloy composition. With 3% HCl at 100 °C (212 °F) and a range of alloy compositions, the rate of attack was as low as 0.36 mpy and as high as 3.3 mpy. At 25 °C (77 °F) and 7M solution, titanium-nickel-iron alloys can lose up to 457 mpy.

**Nitric acid** ( $\text{HNO}_3$ ) is more aggressive toward titanium-nickel than type 304 stainless steel. At 30 °C (86 °F), 10%  $\text{HNO}_3$  attacks at a rate of  $2.5 \times 10^{-2}$  mpy; 60% solution attacks at 0.25 mpy; 5%  $\text{HNO}_3$  at its boiling point attacks at 2 mpy.

**Biocompatibility** studies have been conducted in various media chosen to simulate the conditions of the mouth and the human body. In general, no corrosion of titanium-nickel alloys has been reported. For example, in tests where coupons of titanium-nickel were sealed at 37 °C (97 °F) for 72 h, the mass corrosion rate was on the order of  $10^{-5}$  mpy for such media as synthetic saliva, synthetic sweat, 1% NaCl solution, 1% lactic acid, and 0.1%  $\text{HNaSO}_4$  acid (Ref 29); see also Ref 30.

in excess of 20 ppm by weight can be considered detrimental to ductility, with levels in excess of 200 ppm severely impairing. Under certain conditions,

## 1040 / Advanced Materials

hydrogen can be absorbed during pickling, plating, and caustic cleaning. The exact conditions required for hydrogen absorption are not well defined, so it is advisable to exercise care when performing any of these operations.

Substantial amounts of hydrogen also can be

absorbed in hydrogenated water at elevated temperatures and pressures, such as would be found in pressurized water reactor primary water systems. Relatively short exposure times have been shown to produce hydrogen levels well in excess of 1000 ppm (Ref 32).

## Thermal Properties

## Heat Capacity

A typical plot of specific heat ( $C_p$ ) versus temperature for a 50.2% Ti alloy (see figure) shows a discontinuity at the  $M_s$  temperature of 90 °C (195 °F) (Ref 3). The peak and onset temperatures for the peaks are often used to characterize the transformation temperatures of an alloy. Care must be taken however, (Ref 33), because the presence of an R-phase prior thermal cycling, and residual stresses from sample cutting can tend to complicate the curves and introduce spurious peaks.

## Latent Heats

The latent heat of the martensitic transformation strongly depends on the transformation temperature and stress rate ( $d\sigma/dT$ ) through the formula

$$d\sigma/dT = \Delta H/(\Delta\epsilon T)$$

Typical values for  $\Delta H$  are 4 to 12 cal/g and values for  $d\sigma/dT$  range from 3 to 10 MPa/°C.

The latent heat of fusion can be expressed as:  $\Delta H = -34,000$  J/mol (Ref 34).

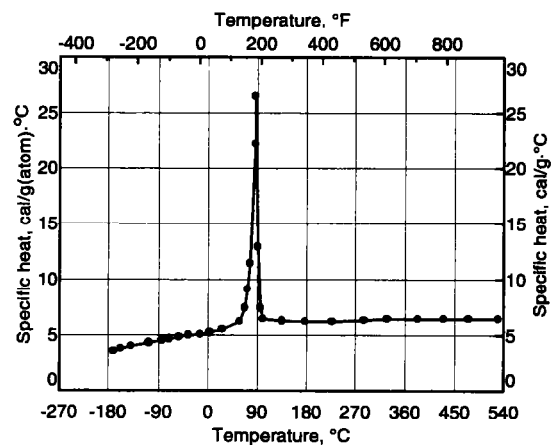
## Thermal Expansion

The thermal coefficient of linear expansion can be expressed as (Ref 23):

$$\alpha \text{ (martensite)} = 6.6 \times 10^{-6}/^\circ\text{C}$$

$$\alpha \text{ (austenite)} = 11 \times 10^{-6}/^\circ\text{C}$$

The volume change on phase transformation ( $\Delta V$ ) (from austenite to martensite) is  $-0.16\%$  (Ref 35).

Specific heat ( $C_p$ )

Specific heat of Ti-49.8Ni (at.%), with a sharp peak in the specific heat at 90 °C (195 °F) corresponding to the  $M_s$  temperature.

Source: C.M. Jackson, H.J. Wagner, and R.J. Wasilewski, NASA Report, NASA-SP 5110, 1972

## Transition Temperatures

## Melting Point

$$T_m = 1310 \text{ }^\circ\text{C} \text{ (2390 }^\circ\text{F)}$$

## Martensitic Transformation Temperatures

Characteristic transformation temperatures depend strongly on composition (see table on next page and the previous section on chemistry). Typical hysteresis widths range from 10 °C (18 °F) for certain titanium-nickel-copper alloys, to 40 to 60 °C (72 to 108 °F) for binary alloys, to 100 °C (180 °F) for titanium-nickel-niobium alloys.

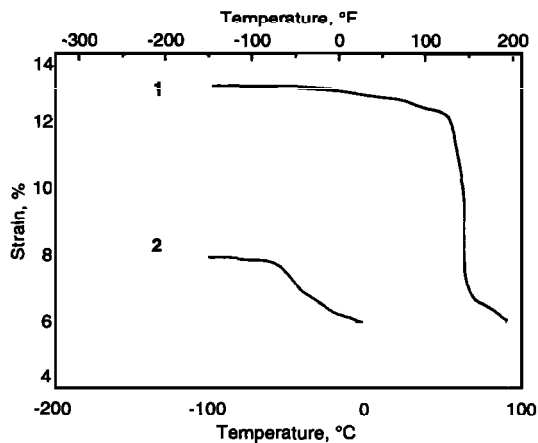
Transformation temperatures are measured by a number of techniques, including electrical resistivity, latent heat of transformation by differential scanning calorimetry, elastic modulus, yield strength, and strain. However, the most useful measurement technique is to monitor the strain on cooling under a constant load and the recovery on heating.

Other important relationships of transforma-

tion temperatures are as follows. Applied stresses increase transformation temperatures according to the stress rate (see the next section on tensile properties). Martensitic deformations increase the stress-free  $A_s$  temperatures, particularly in alloys with low yield stresses. The increase is temporary, returning to the previous value after the first heating cycle. Increasing cold work tends to reduce transformation temperatures. The R-phase transformation temperature is much more constant than those for martensite, typically 20 to 40 °C (68 to 105 °F) in binary alloys.

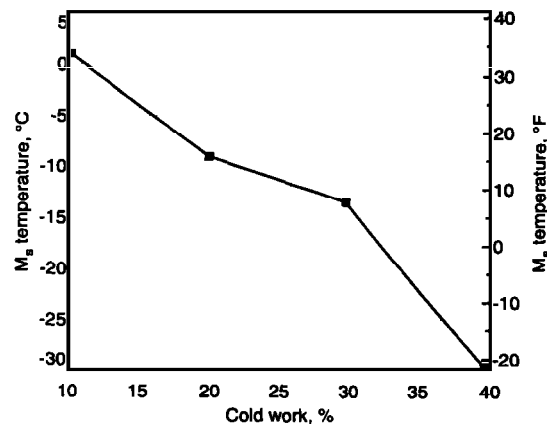
$M_d$ , which is defined as the temperature above which martensite cannot be stress-induced, may be about 25 to 50 °C (50 to 100 °F) higher than  $A_f$ .

Strain of a Ti-Ni-Nb specimen



Strain after deforming and unloading, measured on the first and second heating cycles. Note the change in  $A_s$  and the recovery strain.

Source: K.N. Melton, J.L. Proft, and T.W. Duerig, MRS Int. Meeting on Advanced Materials, Vol 9, K. Otsuka and K. Shimizu, Ed., Materials Research Society, 1989, p 165

 $M_s$  temperature as a function of cold working

Change in the  $M_s$  temperature of a Ti-50.6Ni alloy cold worked 9.2 to 40% and subsequently annealed at 500 °C (930 °F) for 30 min. Source: G.R. Zadno and T.W. Duerig, unpublished research

### Ti-Ni shape memory transformation temperatures

$M_d$ , which is defined as the temperature above which martensite cannot be stress induced, may be about from 25 to 50 °C (50 to 100 °F) higher than  $A_r$ .

Reference(a)	Composition at. % Ni	Temperature, °C				Technique
		$M_s$	$M_r$	$A_s$	$A_r$	
[71 Kor]	46.6	57	12	81	117	Dilatometry
	47.6	37	18	79	134	
	49.6	33	13	75	114	
	50.2	-51	30	33	32	
	51	-136	-178	0	-94	
	51.5	-4	-38	-12	46	
[81 Mel]	52.8	28	-14	44	278	Dilatometry
	49.4	57	5	63	106	
	49.7	20	-20	39	77	
	50.4	-30	-53	-12	0	
[80 Mil]	49.7	45	...	67	...	DTA (as-received material)
	50	44	...	120	...	
	50.1	10	...	52	...	
[68 Wan]	50.5	-9, -29	-29	...	21	Electrical, magnetic properties
	51	20 to 25	...	60	...	
[79 Che]	48.1	100	60	123	140	Electrical resistivity
	48.6	101	74	178	153	
	49.0	66	16	56	93	
	49.5	47	19	53	80	
	50.5	5	-31	8	44	
	51.0	-52	-85	-39	-34	

Compilation from *Phase Diagrams of Binary Titanium Alloys*, (J.L. Murray, Ed.), ASM International, 1987, p 203. (a) Cited references are as follows: 71 Kor: I.I. Kornilov, Ye. V. Kachur, and O.K. Belousov, "Dilatation Analysis of Transformation in the Compound TiNi," *Fiz. Met. Metalloved.*, 32(2), 420-422 (1971) in Russian; TR: *Phys. Met. Metallogr.*, 32(2), 190-193 (1971). 81 Mel: K.N. Melton and O. Mercier, "The Mechanical Properties of NiTi-Based Shape Memory Alloys," *Acta Metall.*, 29, 393-398 (1981). 80 Mil: R.V. Milligan, "Determination of Phase Transformation Temperatures of TiNi Using Differential Thermal Analysis," *Titanium '80, Ti Sci. Tech., Proc. Int. Conf. Kyoto, Japan, May 18-22, T. Kimuzi, Ed.*, 1461-1467 (1980). 68 Wan: F.E. Wang, B.F. DeSavage, and W.J. Buehler, "The Irreversible Critical Range in the TiNi Transition," *J. Appl. Phys.*, 39(5), 2166-2175 (1968). 79 Che: D.B. Chernov, Yu.I. Paskal, V.E. Gyunter, L.A. Monasevich, and E.M. Savitskii, "The Multiplicity of Structural Transitions in Alloys Based on TiNi," *Dokl. Akad. Nauk SSSR*, 247, 854-857 (1979) in Russian; TR: *Sov. Phys. Dokl.*, 24(8), 664-666 (1979)

Tensile Properties

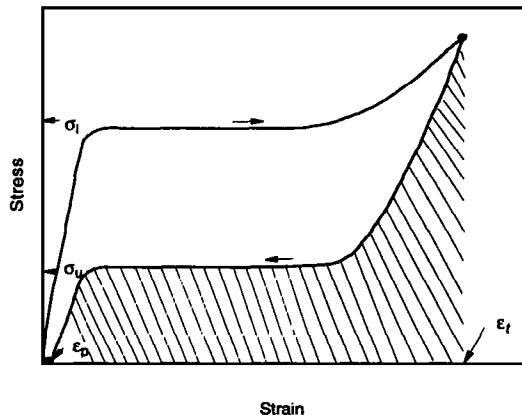
In general, a superelastic curve is characterized by regions of nearly constant stress upon loading (referred to the loading plateau stress) and unloading (unloading plateau stress). These plateau stress values are better indicators of mechanical strength than the traditional yield stress. Typical values are shown (see table).

**Ti-Ni shape memory: Typical loading and unloading characteristics**

Loading plateau	450 to 700 MPa
Unloading plateau	Up to 250 MPa
Maximum springback	11%
Maximum deformation with permanent set	6%
Maximum stored energy	40-50 J/cm <sup>3</sup>

Source: T.W. Duerig and G.R. Zadno, *Engineering Aspects of Shape Memory Alloys*, T.W. Duerig et al., Ed., Butterworth-Heinemann, London, 1990, p 369

**Schematic of superelasticity descriptors**



Schematic diagram showing key descriptors of superelasticity:  $\sigma_u$  (unloading plateau measured as the inflection point),  $\sigma_l$  (loading plateau measured as the inflection point),  $\epsilon_t$  (total deformation strain),  $\epsilon_p$  (permanent set, or amnesia) and the stored energy (shaded area).

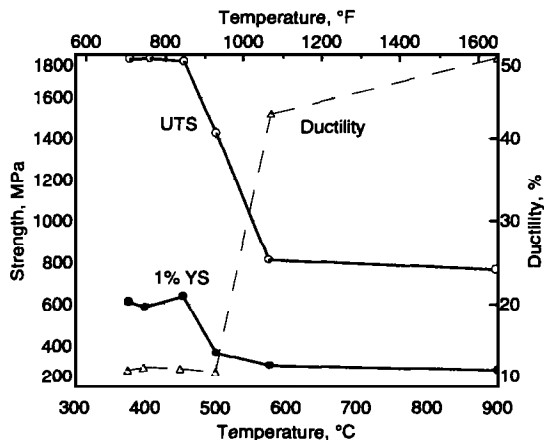
Source: T.W. Duerig and G.R. Zadno, *Engineering Aspects of Shape Memory Alloys*, T.W. Duerig et al., Ed., Butterworth-Heinemann, London, 1990, p 369

**Above  $M_d$**

$M_d$  is defined as the temperature above which martensite cannot be stress-induced. Consequently, titanium-nickel remains austenite throughout an entire tensile test above  $M_d$ . Tensile strengths depend strongly on alloy condition, and the ultimate tensile strength, yield strength, and ductility of cold worked titanium-nickel wire depend on final annealing temperatures (see figure).

Ductility drops sharply as compositions become nickel-rich. A review of other factors controlling ductility can be found in Ref 36.

**Mechanical properties vs anneal temperature**



The influence of annealing temperature on mechanical properties of 0.5 mm (0.02 in.) Ti-50.6Ni wire with 40% cold work and annealed 30 min at temperature.

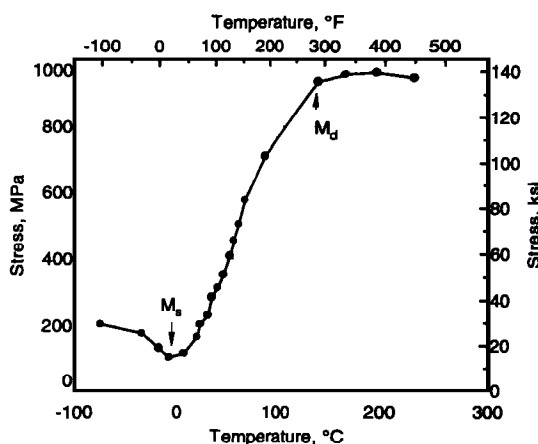
Source: G.R. Zadno and T.W. Duerig, unpublished research

**Below  $M_s$**

Titanium-nickel yield stresses are controlled by the "friction" of the martensite twin interfaces. Typical yields stresses are 120 to 160 MPa (17 to 23 ksi) for binary alloys and as low as 60 to 90 MPa (9

to 13 ksi) for titanium-nickel-copper alloys. Ultimate tensile strengths and ductilities are similar to austenitic values.

**Yield strength vs anneal temperature**



The influence of annealing temperature on mechanical properties of Ti-50.6Ni with 40% cold work annealed 30 min at temperature.

Source: G.R. Zadno and T.W. Duerig, unpublished research

Superelasticity (Between  $M_s$  and  $M_d$ )**Effect of Temperature**

Between  $M_s$  and  $M_d$ , the material transforms from austenite to martensite during tensile testing. Yield strengths vary continuously from  $M_s$  to  $M_d$  (see figure). The rate of stress increase is called the stress rate, varying from 3 to 20 MPa/°C, with rates generally increasing with  $M_s$ .

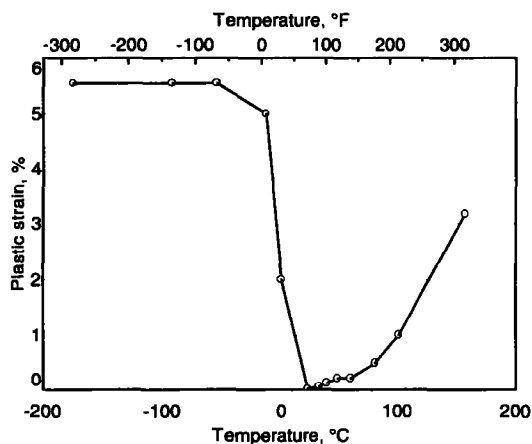
Superelasticity, or pseudoelasticity, is an enhanced elasticity when unloading between  $A_s$  and  $M_d$ . The  $M_d$  transition is generally defined as the temperature above which stress-induced martensite can no longer be formed. On a stress-temperature graph,  $M_d$  is the temperature where the stress begins to level off.

Superelasticity is also highly temperature dependent (see figures). Changing alloy composition and heat treatment can shift the temperature range of superelastic behavior from -100 to +100 °C (-148 to 212 °F).

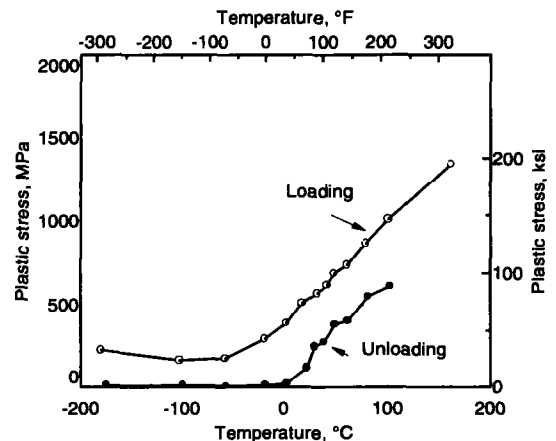
This datasheet describes some of the key properties of equiatomic and near-equiatomic titanium-nickel alloys with compositions yielding

shape memory and superelastic properties. Shape memory and superelasticity *per se* will not be reviewed; readers are referred to Ref 1 to 3 for basic information on titanium-nickel, Tee-nee, Memorite™, Nitinol, Tine™, and Flexon™. These terms do not refer to single alloys or alloy compositions, but to a family of alloys with properties that greatly depend on exact compositional make-up, processing history, and small ternary additions. Each manufacturer has its own series of alloy designations and specifications within the "Ti-Ni" range.

A second complication that readers must acknowledge is that all properties change significantly at the transformation temperatures  $M_s$ ,  $M_f$ ,  $A_s$ , and  $A_f$  (see figure). Moreover, these temperatures depend on applied stress. Thus any given property depends on temperature, stress, and history. Superelasticity is an enhanced elasticity occurring when unloading between  $A_s$  and  $M_d$  (see the section "Tensile Properties" in this datasheet.)

**Permanent set of superelastic wire**

Permanent set of superelastic binary titanium-nickel wire deformed 8.3% and unloaded at various temperatures. Ti-Ni wire with 50.8 at.% Ni cold worked 40% and annealed at 500 °C (930 °F) for 2 min. The superelastic window is roughly 40 °C (70 °F) in width. Source: T.W. Duerig and G.R. Zadno, *Engineering Aspects of Shape Memory Alloys*, T.W. Duerig *et al.*, Ed., Butterworth-Heinemann, London, 1990, p 369

**Loading and unloading plateau heights in Ti-Ni wire**

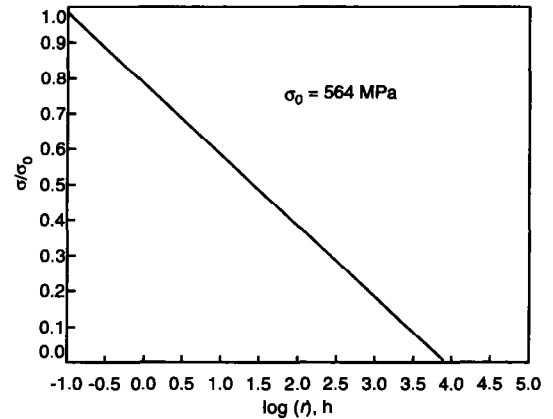
50.8 at.% Ni cold worked 40% and annealed at 500 °C (930 °F) for 2 min. Stress rate = 5.7 MPa/°C. Source: T.W. Duerig and G.R. Zadno, *Engineering Aspects of Shape Memory Alloys*, T.W. Duerig *et al.*, Ed., Butterworth-Heinemann, London, 1990, p 369

## High-Temperature Behavior

**Creep.** Very few creep measurements have been made on titanium-nickel, although creep mechanisms have been proposed (Ref 37).

**Stress relaxation** is critical in many constrained recovery applications. Several measurements have been made (Ref 9, 12, 38). To summarize, relaxation of stable titanium-nickel alloys is extremely slow below 350 °C (660 °F) and becomes very rapid by 425 °C (795 °F).

## Stress relaxation



Stress relaxation of a  $\text{Ni}_{47}\text{Ti}_{50}\text{Fe}_3$  alloy at 375 °C (705 °F) measured in a dynamically controlled creep machine. Round specimens with gage length of 6 mm, fully annealed.

Source: J. Proft and T.W. Duerig, *Engineering Aspects of Shape Memory Alloys*, T.W. Duerig *et al.*, Ed., Butterworth-Heinemann, 1990, p 115

## Fatigue Properties

The fatigue behavior of titanium-nickel alloys is extremely complex and encompasses many different topics. To summarize, titanium-nickel excels in low-cycle, strain-controlled environments, and does relatively poorly in high-cycle, stress-

controlled environments. The superelastic mechanisms accommodate high strains without excessive stresses, but cannot accommodate high stresses without excessively high strains.

### Stress Controlled

Isothermal stress-controlled testing is important in many constrained recovery applications in which the shape memory effect is only used as a mode of installation, e.g., fasteners and couplings, in which the alloys are used exclusively above the  $M_d$  temperature. Although fatigue has been exten-

sively characterized by the coupling and fastener industries, much of the data remains largely unpublished or highly application specific. Typical S-N behavior for various alloy compositions tested well above their  $M_d$  temperatures is shown below (see figure on next page).

### Strain Controlled

Isothermal strain-controlled behavior is highly dependent on the testing temperature relative to the alloy transformation temperature. Fracture follows the Coffin-Manson relationship:

$$N^\beta \Delta \epsilon_p = C$$

where  $C$  and  $\beta$  are constants;  $N$  is the number of cycles to failure; and  $\Delta \epsilon_p$  is the applied strain amplitude (see figure). One specific example of particu-

lar interest is superelastic cycling (strain-controlled testing between  $A_s$  and  $M_d$ ). There are several modes of degradation that occur under these circumstances (see figure). Again, these depend strongly on specific alloy conditions and the needs of the application. Further data are provided in Ref 39.

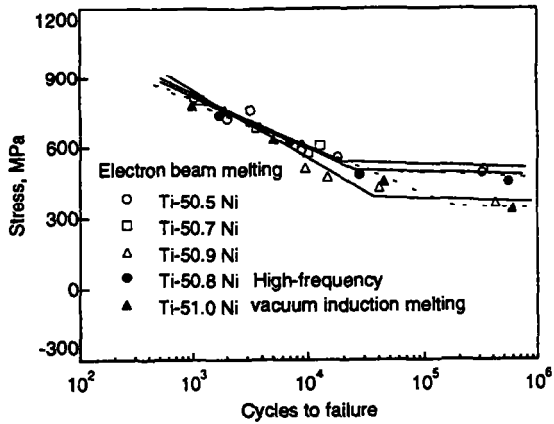
### Thermal Fatigue

Thermal cycling both with and without applied loads such as found in actuators or heat engines, is certainly the most complex mode to analyze. Although it has been studied extensively, it remains difficult to predict failure, largely because failure can consist of fracture, ratcheting, migration of transformation temperatures, changes in reset force, etc. Moreover, damage accumulation depends on stress, strain, temperature change, heat-

ing methods, heating and cooling rates, and even orientation (horizontal or vertical).

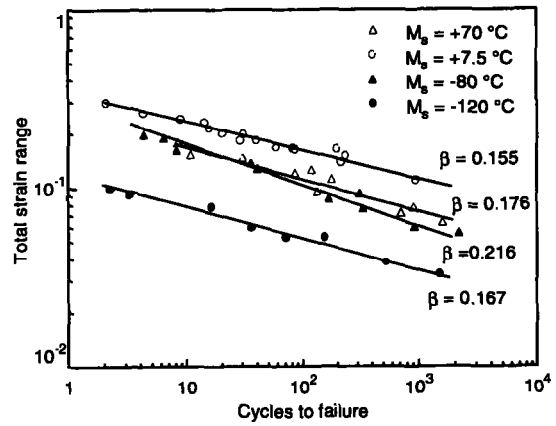
Failure too is nebulous. Various degradation modes can occur, including a shift in transformation temperature, a reduction in the available strain, walking (or ratcheting), and fracture itself. Thermal cycling with no applied load can even result in some degradation. See Ref 40 to 43 for further information.

Typical S-N curves



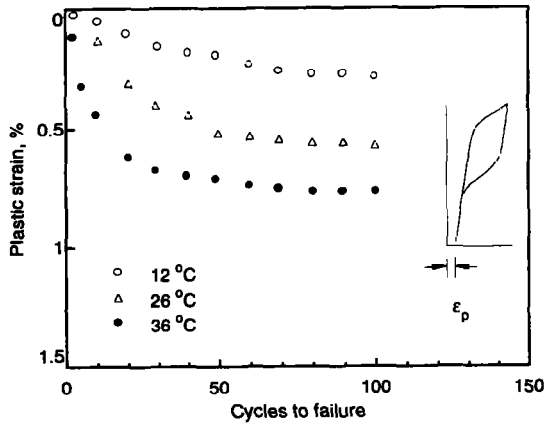
Titanium-nickel alloys of various compositions (at.%) prepared in various fashions is isothermally tested in sheet form. Testing is done well above  $M_s$ . Sheet specimens loaded and unloaded ( $R=0$ ). Cycled at 60 °C (140 °F).  
 Source: S. Miyazaki, Y. Sugaya, and K. Otsuka, MRS Int. Meeting on Advanced Materials, Vol 9, K. Otsuka and K. Shimizu, Ed., Materials Research Society, 1989, p 257

Low-cycle fatigue behavior

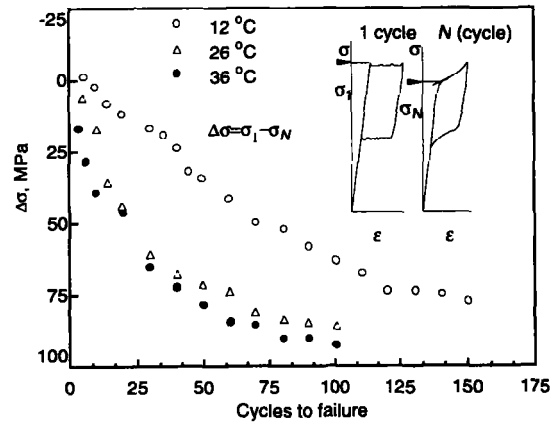


Low-cycle fatigue behavior of titanium-nickel alloys at room temperature tested in tension-compression ( $R = -1$ ). The  $M_s$  temperatures of the alloys are indicated.  
 Source: K.N. Melton and O. Mercier, *Strength of Metals and Alloys*, P. Haasen et al., Ed., Pergamon Press, 1979, p 1246

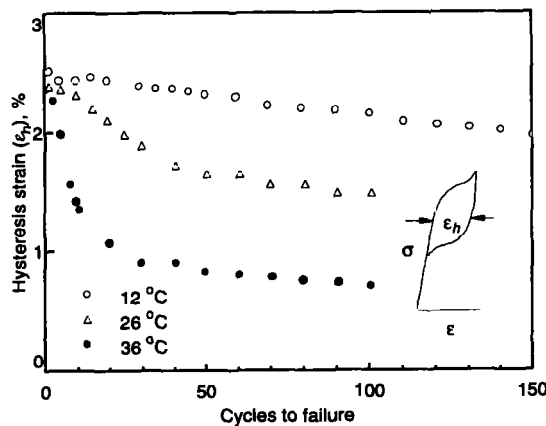
Effects of isothermal superelastic cycling



(a)



(b)



(c)

Tests of a superelastic titanium-nickel wire at three temperatures. Alloy contains 50.6 at.% nickel. Three modes of degradation occur simultaneously during the isothermal superelastic cycling of titanium-nickel alloys: walking, or an accumulation of permanent set (top), a change in yield stress (middle) and a reduction in the hysteresis width (bottom).  
 Source: S. Miyazaki, *Engineering Aspects of Shape Memory Alloys*, T.W. Duerig et al., Ed., Butterworths, 1990, p 403

Fracture

**Fatigue Crack Propagation**

Stress-inducing martensite at the tip of a propagating crack has been shown to significantly

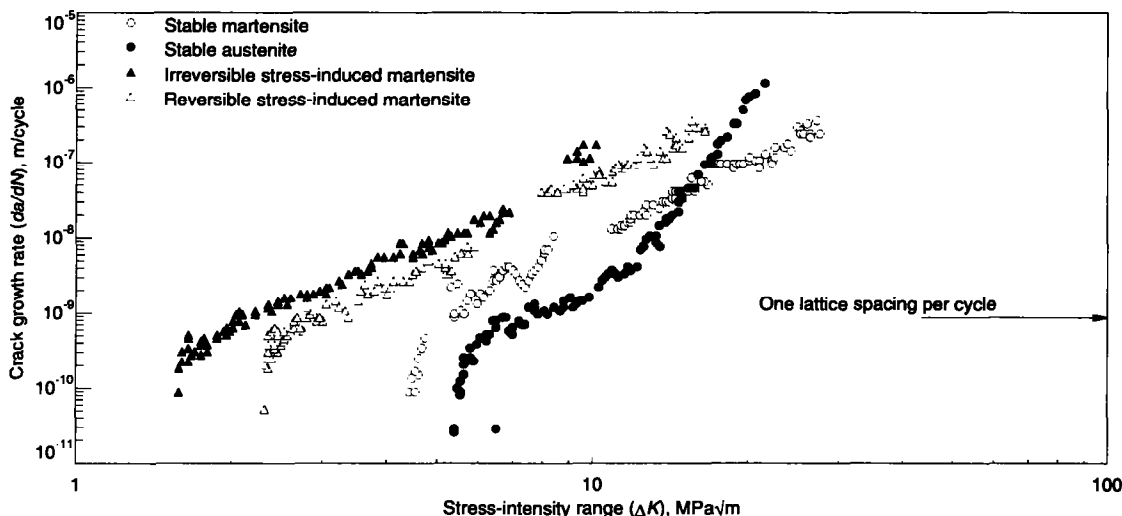
slow crack growth (Ref 44). Other sources of data include Ref 45.

**Toughness**

Although Charpy impact testing on titanium-nickel has been conducted (Ref 3, 46), very little  $K_{Ic}$  or  $J_{Ic}$  data exist. Indications are strong that a

sharp toughness minimum exists at  $M_d$  (see figure).

**Fatigue crack propagation**



Fatigue crack propagation rates in four titanium-nickel alloys, representing *stable martensite* with  $M_s >$  room temperature, *stable austenite* with  $M_s <<$  room temperature, *irreversible stress-induced martensite* with  $M_s <$  room temperature  $< A_s$ , and *reversible stress-induced martensite* with  $A_s <$  room temperature  $< M_s$ . Tested with  $R = 0.1$  on 10 mm thick CT specimens at 50 Hz under conditions of decreasing  $\Delta K$ . Source: R.H. Dauskardt, T.W. Duerig, and R.O. Ritchie, MRS Int. Meeting on Advanced Materials, Vol 9, K. Otsuka and K. Shimizu, Ed., Materials Research Society, 1989, p 243

Processing

**Bulk Working**

**Flow Stress.** Upset forging tests conducted on seven different alloys at strain rates ranging from  $10^{-5}$  to  $10^2$  indicate that the material has a very high hot ductility and is not highly strain rate dependent. The flow stresses can be characterized by the relation:

$$\sigma = k\dot{\epsilon}^m \exp(-Q/RT)$$

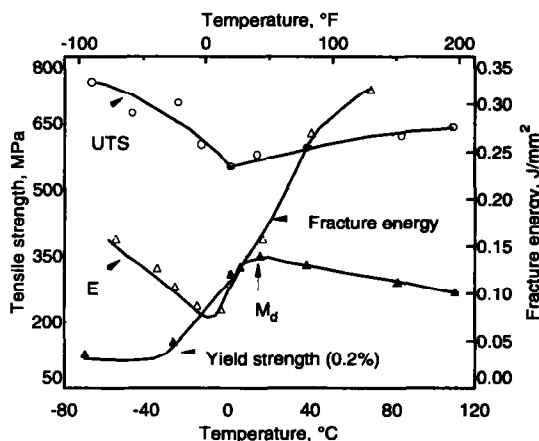
where  $\sigma$  is the flow stress;  $\dot{\epsilon}$  is the strain rate;  $Q$  is an activation energy (50,000 cal/mole); and  $m$  and  $k$  are constants. Values for  $m$  were found to range from 0.1 to 0.17 with increasing temperature (see figure for typical data of an equiatomic binary alloy).

**Extrusion.** Both solid bar and large tube (50 mm diameter with 8 mm wall thickness) have been extruded from titanium-nickel. Parameters remain proprietary.

**Forging.** Titanium-nickel has been successfully forged into large cups. Parameters remain proprietary.

**Rolling.** Titanium-nickel can be hot rolled with relative ease, but is difficult to cold roll, especially in thin, wide sections.

**Fracture energy vs temperature**



Vacuum induction melted alloy hot worked and annealed for 1 h at 950 °C and air cooled. Standard Charpy V-notch impact specimens were machined. The influence of temperature on fracture toughness of 44Ti-49Ni-5Cu-2Fe (wt%). Note that the minimum in the fracture energy occurs just below  $M_d$ , as determined from the corresponding 0.2% yield strength and ultimate tensile strength measurements. Source: K.N. Melton and O. Mercier, *Acta Metall.*, Vol 29, 1982, p 393

**Fabrication**

**Casting.** Although some unreported experiments have been conducted, casting has not been done on a commercial level.

**Powder Metallurgy.** Although a great deal of experimentation has taken place with both elemental and prealloyed powders, nothing has reached near-production levels. Reference 5 provides a review of methods.

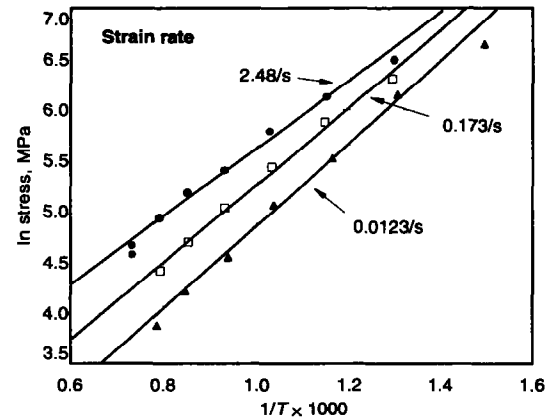
**Forming.** Titanium-nickel sheet has been successfully formed into a range of complex shapes, both in the martensite and austenitic phases. Springback is high, as is die wear and friction. Parameters remain proprietary.

**Machining.** Titanium-nickel is very difficult to machine. Very low speeds and a great deal of coolant is required, and tool wear is very rapid. Milling and drilling are particularly difficult. Producers of couplings have demonstrated that large-scale machining production is possible.

**Heat Treatment.** Titanium-nickel can be heat treated in air up to ~500 °C (930 °F). No  $\alpha$  case is formed, but a surface oxide of rutile develops quickly. Above 500 °C (930 °F), the oxide layer begins to flake (depending on time). Nitrogen and hydrogen atmospheres are not recommended. Argon, helium, and vacuum heat treatments are commonly used to preserve bright finishes.

Recrystallization is extremely rapid above 700 °C (1290 °F). Solution treatment requires temperatures of at least 550 °C (1020 °F). Stress relief is usually accomplished at temperatures as low as 300 °C (570 °F). A TTT diagram is shown in the previous section "Phases and Structures."

Fully annealed bar stock has a typical hardness of 60 HRA. Vicker numbers range from 190 HV in the annealed condition to 240 HV after 15% cold work (Ref 3).

**Flow stress measurements**

Natural log (ln) of flow stress is shown to vary linearly with the inverse of absolute temperature. 12 mm x 8 mm diameter specimens tested in compression under isothermal conditions (heated dies) at the temperatures and strain rates shown. Source: T.W. Duerig, unpublished data

**Joining.** Titanium-nickel is difficult to join because most mating materials cannot tolerate the large strains experienced by the alloy. Most applications rely on crimped bonds. It can be welded to itself with relative ease by resistance and TIG methods. Welding to other materials is extremely difficult, although proprietary methods do exist and are practiced in large volumes in the production of eyeglass frames.

Brazing can only be accomplished after re-enforcement and plating. Again, methods are proprietary; large-scale production is practiced by the eyeglass frame industry.

**References**

1. T.W. Duerig *et al.*, Ed., *Engineering Aspects of Shape Memory Alloys*, Butterworth-Heinemann, London, 1990
2. J. Perkins, Ed., *Shape Memory Effects in Alloys*, Plenum Press, 1975
3. C.M. Jackson, H.J. Wagner, and R.J. Wasilewski, NASA Report, NASA-SP 5110, 1972
4. J. Takahashi, M. Okazaki, K. Hiroshi, and Y. Furuta, private communication, 1984
5. T.W. Duerig, in *Advanced Synthesis of Materials*, J. Moore, Ed., 1993, to be published
6. G.R. Zadno and T.W. Duerig, *Engineering Aspects of Shape Memory Alloys*, T.W. Duerig *et al.*, Butterworth-Heinemann, London, 1990, p 414
7. M. Nishida, C.M. Wayman and T. Honma, *Metall. Trans. A*, Vol 17, 1986, p 1505
8. T.W. Duerig and K.N. Melton, Proc. of SMA'86, C. Youyi *et al.*, Ed., China Academic Publishers, 1986, p 397
9. J.L. Proft and T.W. Duerig, *Engineering Aspects of Shape Memory Alloys*, T.W. Duerig *et al.*, Butterworth-Heinemann, London, 1990, p 115
10. A. Keeley, D. Stöckel, and T.W. Duerig, *Engineering Aspects of Shape Memory Alloys*, T.W. Duerig *et al.*, Ed., Butterworth-Heinemann, London, 1990, p 181
11. T.W. Duerig and G.R. Zadno, *Engineering Aspects of Shape Memory Alloys*, T.W. Duerig *et al.*, Ed., Butterworth-Heinemann, London, 1990, p 369
12. C.R. Such, "The Characterization of the Reversion Stress in NiTi," M.S. Thesis, Naval Post Graduate School, Monterey, CA, 1974
13. M.V. Nevitt, *Trans. Met. Soc. AIME*, Vol 218, 1960, p 327
14. D.M. Goldstein, W.J. Buehler, and R.C. Wiley, Effects of Alloying upon Certain Properties of 55.1 Nitinol, NOLTR 64-235, 1964
15. H.K. Eckelmeyer, Sandia Labs Report 74-0418, 1974
16. D.B. Chernov *et al.*, *Dokl. Akad. Nauk. SSSR*, Vol 245 (No. 2), 1979, p 360
17. P.G. Lindquist and C.M. Wayman, *Engineering Aspects of Shape Memory Alloys*, T.W. Duerig *et al.*, Butterworth-Heinemann, London, 1990, p 58
18. T.W. Duerig and K.N. Melton, *The Martensite Transformation in Science and Technology*, E. Hornbogen and H. Jost, Ed., Deutsche Gesellschaft für Metallkunde, Germany, 1988, p 191
19. W. Moberly and K. Melton, *Engineering Aspects of Shape Memory Alloys*, T.W. Duerig *et*

## 1048 / Advanced Materials

- al.*, Ed., Butterworth-Heinemann, London, 1990, p 46
20. O. Matsumoto, S. Miyazaki, K. Otsuka, and H. Tamura, *Acta Metall.*, Vol 35, 1987, p 2137
  21. H.C. Ling and R. Kaplow, *Metall. Trans. A*, Vol 12, 1981, p 2101
  22. L. Kaufman, S.A. Kulin, P. Neshe, and R. Salzbrenner, *Shape Memory Effects in Alloys*, J. Perkins, Ed., Plenum Press, 1975, p 547
  23. S. Spinner and A.G. Rozner, *J. Acoust. Soc. Am.*, Vol 40, 1966, p 1009
  24. R.J. Wasilewski, *Trans. AIME*, Vol 233, 1965, p 1691
  25. O.K. Belousov, *Russ. Metall.*, Vol 2, 1981, p 204
  26. J.E. Hanlon, S.R. Butler, and R.J. Wasilewski, *Trans. AIME*, Vol 239, 1967, p 1323
  27. C-M. Chan, S. Trigwell, and T.W. Duerig, *Surf. Interface Anal.*, Vol 15, 1990, p 349
  28. J.D. Harrison, Raychem Report, 1991
  29. S. Lu, *Engineering Aspects of Shape Memory Alloys*, T.W. Duerig *et al.*, Ed., Butterworth-Heinemann, London, 1990, p 445
  30. L.S. Castleman, S.M. Motzkin, F.P. Alicandri, V.L. Bonawit, and A.A. Johnson, *J. Biomed. Mater. Res.*, Vol 10, 1976, p 695
  31. R. Burch and N.B. Mason, *J.C.S. Faraday I*, Vol 75, 1979, p 561; R.B. Burch and N.B. Mason, *J.C.S. Faraday I*, Vol 75, 1979, p 578
  32. A.R. Pelton and T.W. Duerig, "An Analysis of Crofit Couplings After One-Year Service at Seabrook," Raychem Proprietary Report, 1991
  33. G. Airoldi and B. Rivolta, *Phys. Scripta*, Vol 37, 1988, p 891
  34. J.C. Gachon and J. Hertz, *CALPHAD*, Vol 7, 1983, p 1
  35. K. Otsuka, T. Sawamura, K. Shimizu, and C.M. Wayman, *Metall. Trans.*, Vol 2, 1971, p 2583
  36. S. Miyazaki *et al.*, *Mater. Sci. Forum*, Vol 56-58, 1990, p 765
  37. A.K. Mukherjee, *J. Appl. Phys.*, Vol 39 (No. 5), 1968, p 2201
  38. A. Terui *et al.*, *Nip. Kikai Gakkai Ronbunshu, A. Hen*, Vol 51 (No. 462), 1985, p 488
  39. G.R. Zadno, W. Yu, and T.W. Duerig, *Materials Science Forum*, Vol 56-58, B.C. Muddle, Ed., 1990, p 771
  40. H. Tamura, Y. Suzuki and T. Todoroki, Proc. Int. Conf. Martensitic Transformations, Japan Institute of Metals, 1986, p 736
  41. Y. Furuya *et al.*, MRS Int. Meeting on Advanced Materials, Vol 9, K. Otsuka and K. Shimizu, Ed., Materials Research Society, 1989, p 269
  42. Y. Suzuki and H. Tamura, *Engineering Aspects of Shape Memory Alloys*, T.W. Duerig *et al.*, Ed., Butterworth-Heinemann, London, 1990, p 256
  43. J.L. Proft, K.N. Melton, and T.W. Duerig, MRS Int. Meeting on Advanced Materials, Vol 9, K. Otsuka and K. Shimizu, Ed., Materials Research Society, 1989, p 159
  44. R.H. Dauskardt, T.W. Duerig, and R.O. Richie, MRS Int. Meeting on Advanced Materials, Vol 9, K. Otsuka and K. Shimizu, Ed., Materials Research Society, 1989, p 251
  45. S. Miyazaki, Y. Sugaya, and K. Otsuka, MRS Int. Meeting on Advanced Materials, Vol 9, K. Otsuka and K. Shimizu, Ed., Materials Research Society, 1989, p 251
  46. K.N. Melton and O. Mercier, *Acta Metall.*, Vol 29, 1982, p 393